

1    Population genetic inferences using immune gene SNPs mirror  
2                                    patterns inferred by microsatellites

3                                    JEAN P. ELBERS<sup>1,3</sup>, RACHEL W. CLOSTIO<sup>2</sup>, SABRINA S. TAYLOR<sup>1</sup>

<sup>1</sup>School of Renewable Natural Resources, 227 RNR Bldg., Louisiana State University and AgCenter,  
Baton Rouge, Louisiana, 70803, USA

<sup>2</sup>Department of Biology, 300 E. St. Mary Blvd., University of Louisiana at Lafayette,  
Lafayette, Louisiana, 70503, USA

Keywords: microsatellites, target enrichment, sequence capture,  
next-generation sequencing, immunogenetics, population genomics

<sup>3</sup>Corresponding author: Fax: 225-578-4227, Email: [jean.elbers@gmail.com](mailto:jean.elbers@gmail.com)

Running title: Immune gene SNPs mirror microsatellites

## Abstract

Single nucleotide polymorphisms (SNPs) are replacing microsatellites for population genetic analyses, but it is not apparent how many SNPs are needed or how well SNPs correlate with microsatellites. We used data from the gopher tortoise, *Gopherus polyphemus* - a species with small populations, to compare SNPs and microsatellites to estimate population genetic parameters. Specifically, we compared one SNP dataset (16 tortoises from 4 populations sequenced at 17,901 SNPs) to two microsatellite datasets, a full dataset of 101 tortoises and a partial dataset of 16 tortoises previously genotyped at 10 microsatellites. For the full microsatellite dataset, observed heterozygosity, expected heterozygosity, and  $F_{ST}$  were correlated between SNPs and microsatellites; however, allelic richness was not. The same was true for the partial microsatellite dataset, except that allelic richness, but not observed heterozygosity, was correlated. The number of clusters estimated by Structure differed for each dataset (SNPs = 2; partial microsatellite = 3; full microsatellite = 4). PCA showed four clusters for all datasets. More than 800 SNPs were needed to correlate with allelic richness, observed heterozygosity, and expected heterozygosity, but only 100 were needed for  $F_{ST}$ . The number of SNPs typically obtained from NGS far exceeds the number needed to correlate with microsatellite parameter estimates. Our study illustrates that diversity,  $F_{ST}$ , and PCA results from microsatellites can mirror those obtained with SNPs. These results may be generally applicable to small populations, a defining feature of endangered and threatened species, because theory predicts that genetic drift will tend to outweigh selection in small populations.

## Introduction

Molecular markers vary in their utility and application to population genetic studies, and geneticists use available markers suited to answering questions at hand. Initially, geneticists only had allozymes and used them to infer nucleotide changes underlying differences in protein migration during electrophoresis. Later, variable mitochondrial DNA markers were used because of the availability of conserved primers and the high copy number of mitochondria, but mitochondrial markers mostly provided information on broad-scale genetic patterns (Moritz, 1994). Presently, markers such as microsatellites are commonly used in population genetics because most are presumed neutral, are found throughout genomes, and can elucidate fine-scale spatial genetic patterns (e.g., Clostio *et al.*, 2012).

Genomic resources, hybridization arrays, fluorescent probes, and next-generation sequencing (NGS) have allowed researchers to access other types of genomic markers, and recently large arrays of single nucleotide

polymorphisms (SNPs) have become particularly popular in population genetic studies of not only model but also non-model organisms (Allendorf *et al.*, 2010). SNPs are one of the most numerous molecular markers (Gupta *et al.*, 2001), and thousands to millions of them can be examined simultaneously using NGS techniques compared to dozens observed in traditional Sanger sequencing-based approaches. However, as the preferred tool shifts from microsatellites to genome-wide SNPs, it is important to understand new results in the context of previous research.

Prior research has shown that microsatellite-derived population genetic parameters generally correlate with parameters derived from SNPs. Most data from pre-NGS SNP methods find correlations between microsatellites and SNPs (e.g., Ryyanen *et al.*, 2007; Narum *et al.*, 2008; Coates *et al.*, 2009; Glover *et al.*, 2010; Garke *et al.*, 2012), but there are some exceptions (e.g., Vali *et al.*, 2008; DeFaveri *et al.*, 2013). Considerably fewer studies have compared genetic inferences derived from microsatellites to inferences from thousands of NGS generated SNPs, but there are some examples from restriction site-associated DNA sequencing (RADseq) studies where correlations are present (Jeffries *et al.*, 2016) between the two types of markers for population genetic parameters or not (Lozier, 2014). As more and more studies use NGS data, a better understanding of this relationship is imperative because many current management and recovery plans currently in effect are based on genetic data from microsatellites, and these plans may change if results from microsatellites and NGS data are consistently and substantively different.

Although microsatellites are frequently presumed to be neutral because they are not transcribed or translated, they can be linked to functional genes under selection (e.g., Vasemagi *et al.*, 2005; Li *et al.*, 2014) or may be involved in DNA folding (Li *et al.*, 2002). SNPs can be influenced by either neutral or adaptive genetic processes and can represent functional, coding regions of the genome, which on the one hand are under purifying selection to avoid deleterious changes and on the other under positive selection for advantageous changes. For example, SNPs present in genes that influence immune response are likely to be under strong positive selection as such changes could provide resilience to infectious disease (Bernatchez & Landry, 2003; Sommer, 2005). Additionally, SNPs in immune genes may be under balancing selection to maintain polymorphisms in populations (e.g., Niskanen *et al.*, 2014) by types of balancing selection such heterozygote advantage, frequency-dependent selection, and variable selection in time and space (Hedrick, 1999).

Although genes such as immune genes are predicted to be under strong selective pressure, neutral genetic processes affect the entire genome, including genes under selection, even when selection is the main evolutionary force (Kuo *et al.*, 2009; Lynch *et al.*, 2011). However, when effective population sizes ( $N_e$ ) are small, genes influenced by selection may behave like effectively neutral loci because genetic drift tends to outweigh

selection in small populations (e.g., Grueber *et al.*, 2013; Miller & Lambert, 2004). In particular, loci under selection may be effectively neutral if their selection coefficient ( $s$ ) is less than or equal to  $(1/(2N_e))$  (Wright, 1931). For example, for alleles of immune response genes such as those of the major histocompatibility complex (MHC), which can have high selection coefficients of 1%, such alleles could behave like effectively neutral loci if effective population sizes are less than 50 individuals (Frankham *et al.*, 2010). Empirical studies support these conclusions as MHC loci behave like effectively neutral loci for a variety of threatened vertebrates with small, bottlenecked populations (Weber *et al.*, 2004; Miller *et al.*, 2008; Taylor *et al.*, 2012).

We recently applied genomic approaches to the threatened (gopher tortoise) *Gopherus polyphemus* by isolating genes involved in immune responses to better understand susceptibility to a chronic and occasionally fatal infectious upper respiratory tract disease (Elbers & Taylor, 2015). These samples were also previously genotyped at 10 microsatellites by Clostio *et al.* (2012) providing an excellent opportunity to compare population genetic parameters derived from presumably neutrally evolving microsatellites and presumably drift and/or selection-influenced immune gene SNPs from an organism with generally small population sizes.

We leveraged the NGS (Elbers & Taylor, 2015) and microsatellite (Clostio *et al.*, 2012) data already collected for *G. polyphemus* to compare estimates of population genetic diversity, differentiation, and admixture derived from immune gene SNPs and microsatellites using samples from the same populations to better understand how NGS SNP inferences relate to those from microsatellites. We also subsample our SNPs to determine how many are needed to replace a given number of microsatellites for estimating genetic diversity and differentiation. Although immune gene SNPs are putatively under selection and microsatellites are presumably neutral, we predict inferences from immune gene SNPs will mostly correlate with microsatellite inferences as there will be a preponderance of selectively neutral immune gene SNPs due to the generally small population sizes of *G. polyphemus*. We also predict that not all of the discovered SNPs will be needed to replace microsatellites for estimating diversity and differentiation.

## Methods

### Samples

Because SNP analyses are often costly, smaller sample sizes than those used in microsatellite studies are typical. In this study we were interested in how a smaller sample size but a larger number of SNP markers would compare to a typical microsatellite dataset. We were limited to analyzing SNPs from 16 tortoises, so we randomly chose 16 *G. polyphemus* from 4 sample populations (4 per population, Fig. 1). These 4

sample populations were chosen out of the 24 used by Clostio *et al.* (2012) because they were distributed along an east to west gradient and were likely representative of the genetic variability for the species. We compared the SNP dataset to two microsatellite datasets: (1) the full microsatellite dataset of 101 tortoises sampled by Clostio *et al.* (2012) (Table 1); and, (2) a partial microsatellite dataset of 16 tortoises. We used two microsatellite datasets to: 1) equalize sample size (partial), and ; 2) use a sample size representative of a typical microsatellite study (full). Only 1 GA tortoise in the SNP dataset had been previously genotyped at all 10 microsatellite loci by Clostio *et al.* (2012), so for the partial microsatellite dataset, we randomly chose 3 additional tortoises from the GA population that had been genotyped at all 10 microsatellites. Thus, the SNP dataset and the partial microsatellite dataset only differed by 3 samples from the GA population.

## Target region for sequencing SNPs

The methods for acquiring SNP data are presented in Elbers & Taylor (2015). Briefly, we created a target region to capture the immunome (i.e., genes involved in immune response, *sensu amplo* Ortutay & Vihinen (2006)) of *Chrysemys picta bellii* (western painted turtle) using the GO2TR workflow (Elbers & Taylor, 2015). The workflow filtered the *C. p. bellii* 3.0.1 genome assembly (Shaffer *et al.*, 2013) annotated by the NCBI Eukaryotic Genome Annotation Pipeline (annotation release 100) using the gene ontology term "immune response" (i.e., genes that function in the immune system's response to internal or invasive threats). Jean-Marie Rouillard of MYcroarray Inc. (Ann Arbor, MI, USA) generated 120-bp bait sequences with 60-bp overlap to capture our 1.4Mbp target region.

## Library preparation and sequence capture

We used biotinylated RNA baits from MYcroarray in an in-solution hybridization experiment to capture the immunomes of 16 *G. polyphemus*. We created 16 Illumina adaptor-ligated libraries using Agilent Sure-Select XT2 Reagent Kits for the Illumina MiSeq (Agilent Technologies, Santa Clara, CA, USA), pooled 16 prepared libraries per capture reaction, and used MYcroarray reagents and protocols for sequence capture. We then sequenced post-capture amplification libraries on two Illumina MiSeq sequencer flow cells (i.e., all individuals sequenced twice) using MiSeq version 3 chemistry and 75-bp paired-end reads at Pennington Biomedical Research Center (Baton Rouge, LA, USA).

## 119 Read quality control and mapping

120 We demultiplexed reads for each MiSeq run, allowing for up to one mismatch in the 8-bp barcode using  
121 MiSeq Reporter software. We used TRIMMOMATIC v0.32 (Bolger *et al.*, 2014) default settings for adapter  
122 trimming, and for base quality filtering, we trimmed leading and trailing bases with quality scores less than  
123 5 and 15, respectively. We also used sliding window scans to remove the 3' end of reads when average quality  
124 dropped below 15, and discarded reads with less than 40 bases. We next merged overlapping paired-ends  
125 reads with BBMerge v5.4 from the BBMap suite (<https://sourceforge.net/projects/bbmap/>) and then  
126 combined unpaired single reads (n=9.08 million) and merged paired reads for downstream analysis. Paired  
127 and single plus merged reads were first mapped separately to the *C. p. bellii* 3.0.3 genome using the BWA-MEM  
128 algorithm (Li, 2013) implemented in BWA v0.7.12 (Li & Durbin, 2009), and then less stringently using STAMPY  
129 v1.0.23 (Lunter & Goodson, 2011). We used SAMTOOLS v1.1 (Li *et al.*, 2009) to merge binary alignment map  
130 (BAM) files from paired reads and single plus merged reads. NCBI remap ([http://www.ncbi.nlm.nih.gov/](http://www.ncbi.nlm.nih.gov/genome/tools/remap)  
131 [genome/tools/remap](http://www.ncbi.nlm.nih.gov/genome/tools/remap)) was used to convert our bait intervals from *C. p. bellii* 3.0.1 to *C. p. bellii* 3.0.3  
132 coordinates.

## 133 Variant and genotype calling

134 Mapped reads were then processed using the Genome Analysis Toolkit v3.3.0 (McKenna *et al.*, 2010,  
135 GATK), adhering to GATK best practices for exome sequencing and calling variants such as SNPs with GATK's  
136 Haplotype Caller and Unified Genotyper.

137 We then filtered variants to remove those with bad validation, low quality, low read depth, or low genotype  
138 quality to produce a high quality set of SNPs called by the Unified Genotyper. Next, we called variants  
139 from base-recalibrated BAM files using the Haplotype Caller and filtered variants in the same manner  
140 as before. We then looked for concordance between the two variant callers and used concordant SNPs for  
141 variant quality filtering of the Haplotype Caller's call set. Finally, we used BEAGLE v4.0 r1398 (Browning  
142 & Browning, 2007) for genotype imputation on the variant-recalibrated SNP set. Following variant calling,  
143 we used PICARD's v1.128 (<http://broadinstitute.github.io/picard/>) CalculateHSMetrics to estimate  
144 sequencing metrics, and featureCounts (Liao *et al.*, 2014) to estimate the number of genes and exons covered  
145 by each sample.

## Population genomic analyses

For all population genomic analyses, we analyzed only di-allelic polymorphic SNP loci, as the tri- ( $n=758$ ) and tetra-allelic ( $n=7$ ) loci we obtained would influence SNP heterozygosity estimates. We used **VCFT00LS** v0.1.12b (Danecek *et al.*, 2011) to recalculate allele frequencies from our **Beagle**-imputed SNPs and then removed loci with allele frequencies of one. We then pruned SNP loci that were out of Hardy-Weinberg Equilibrium (HWE) or in Linkage Disequilibrium (LD) within each population using default settings in **VCFT00LS**. We used the `p.adjust` function in **R** (R Core Team, 2015) to correct  $P$  values for HWE and LD tests using a false discovery rate (Benjamini & Hochberg, 1995) of 0.05.

We examined what polymorphic SNPs might be under selection with **BayeScan** v2.1 (Foll & Gaggiotti, 2008) with the intent of pruning those SNPs that were putatively under selection. We used the `make_bayescan_input.py` script to convert variant call format (VCF) to **BayeScan** input format (De Wit *et al.*, 2012) and a false discovery rate of 0.05. In order for a given SNP to be included in the analysis, we required at least four good quality genotypes from each population and at least one copy of the minor allele for a locus.

For genetic diversity analyses and all subsequent file conversions, we used **PGDSpider** v2.0.7.4 (Lischer & Excoffier, 2012) and the **R** package **hierfstat** v0.04-10 (Goudet, 2005) to assess observed and expected heterozygosity and allelic richness. For population genomic differentiation, we estimated  $F_{ST}$  values with **hierfstat**. For estimating admixture, we performed principle component analyses (PCA) with **hierfstat**, and we also assessed population admixture using **STRUCTURE** v2.3.4 (Pritchard *et al.*, 2000; Hubisz *et al.*, 2009). We ran **STRUCTURE** with 100,000 burnins and 1,000,000 replicates using correlated allele frequency and the admixture ancestry models from  $K=1-5$  with 20 replicates per  $K$  value. We used **STRUCTURE HARVESTER** web v0.6.94 (Earl & vonHoldt, 2012) to select the best  $K$  value and **CLUMPAK** web server (Kopelman *et al.*, 2015) to average data from multiple runs and to visualize population assignments.

## Microsatellite analyses

We assessed HWE and LD for the full and partial microsatellite datasets using **ARLEQUIN** v3.5 (Excoffier & Lischer, 2010). All 10 loci for both datasets were in HWE and linkage equilibrium. Genetic diversity, differentiation, and admixture were estimated in the same manner as SNPs using **hierfstat** and **STRUCTURE**.

## 173 Random sampling of SNPs for subsampling analysis

174 We examined how many SNP loci would be needed to obtain  $P$  values  $< 0.05$  for Pearson's  $r$  correlation  
175 coefficient with the full and partial microsatellite datasets for allelic richness, heterozygosities, and  $F_{ST}$  values  
176 by randomly subsampling our 17,901 SNPs. We did not include allelic richness when comparing the SNP and  
177 full microsatellite datasets because they were not correlated at the 0.05 level, and we did not include allelic  
178 richness and observed heterozygosity when comparing the SNP and partial microsatellite datasets because  
179 they were not correlated. We randomly chose SNPs among the following sample sizes using a custom R script:  
180 10, 20, 40, 100, 200, 400, 800, 1,600, 3,200, 6,400, or 13,200 SNPs and calculated the  $P$  value of the Pearson's  
181 correlation coefficient using the `cor.test` function in R for each sample size of SNP loci for allelic richness,  
182 observed heterozygosity, expected heterozygosity, and  $F_{ST}$ . We repeated the process and chose 10 replicates  
183 for each sample size for both the full and partial microsatellite datasets.

## 184 Effective population size

185 We estimated effective population size using the full microsatellite and SNP datasets with the program  
186 `NeEstimator` v2.01 (Do *et al.*, 2014) and employed one single-sample estimator of  $N_e$  (i.e., the linkage  
187 disequilibrium method of Waples & Do (2008)), and two single-sample estimators of the number of effective  
188 breeders per year (i.e.,  $N_b$  using the heterozygote-excess method of Zhdanova & Pudovkin (2008) and the  
189 molecular coancestry method of Nomura (2008)). We converted  $N_b$  to  $N_e$  by multiplying  $N_b$  by the generation  
190 time of 31 years for the gopher tortoise (Enge *et al.*, 2006).

## 191 Results

192 From two Illumina MiSeq sequencer runs, we obtained 47.5 million reads that passed quality control and  
193 were assignable to individuals. Each tortoise had  $3 \pm 0.7$  (mean  $\pm$  standard deviation) million reads of which  
194  $47.9 \pm 3.2$  % were unique (i.e., were not PCR duplicates), and  $98.8 \pm 0.1$  % of these unique reads could be  
195 aligned to our target region (Table S1, Supporting information). Mean sample coverage over the entire target  
196 region was  $65.4 \pm 13$  reads, and each sample had  $69.3 \pm 3.6$  % target bases with coverage greater than 20  
197 reads (Fig. S2, Fig. S3, Supporting information). Only 4.7 % (66.3 Kbp) of the 1.4 Mbp target region had  
198 coverage of less than 2 reads. Although our target region contained a total of 632 immune genes and 5,425  
199 exons, only 611 genes and 4,837 exons were represented by usable reads. Each sample had reads for  $592.1 \pm$   
200  $4.2$  genes and  $4,106 \pm 98.1$  exons (mean  $\pm$  standard deviation).



201 There were 17,901 di-allelic polymorphic SNP loci after filtering and imputation. None of these loci were  
202 out of HWE or in LD, but the lack of LD is unlikely given the close proximity of loci within the same  
203 exon. This may have occurred because we had to correct  $P$  values to account for thousands of multiple tests.  
204 Polymorphic SNPs were present in 491 immune genes (Table S2, Supporting information) and included broad  
205 classes such as major histocompatibility and Toll-like receptor genes (Table 2).

206 There were 66 SNP loci that may have been under selection, which represented 31 genes. Pruning these  
207 SNPs did not significantly influence results, so we chose to analyze the full SNP dataset when comparing  
208 genetic diversity, differentiation, or admixture between SNPs and microsatellites.

209 SNP allelic richness was not positively correlated with values derived from the full microsatellite dataset  
210 (Fig. 2A, Pearson's  $r = 0.411$ ,  $P = 0.294$ ); however, SNP and microsatellite observed (Fig. 2B, Pearson's  $r$   
211  $= 0.945$ ,  $P = 0.028$ ) and expected heterozygosities (Fig. 2C, Pearson's  $r = 0.976$ ,  $P = 0.012$ ) were highly  
212 correlated. Allelic richness was correlated between the SNP and partial microsatellite datasets (Fig. 2E,  
213 Pearson's  $r = 0.992$ ,  $P = 0.004$ ). Observed heterozygosity was not correlated (Fig. 2F, Pearson's  $r = 0.63$ ,  
214  $P = 0.185$ ), but expected heterozygosity was (Fig. 2G, Pearson's  $r = 0.924$ ,  $P = 0.038$ ). The LA population  
215 followed by FL then GA and AL populations had the lowest to highest heterozygosity and allelic richness for  
216 SNPs. This suggests lower genetic diversity in the western LA population versus eastern FL, GA, and AL  
217 populations based on SNPs, a similar result to that obtained with both microsatellite datasets.

218 Pairwise  $F_{ST}$  values were also positively correlated for SNP and the full (Fig. 2D, Pearson's  $r = 0.96$ ,  $P$   
219  $= 0.001$ ) and partial (Fig. 2H, Pearson's  $r = 0.968$ ,  $P = 0.001$ ) microsatellite datasets. However, LA and  
220 AL had the lowest differentiation for SNPs compared to second lowest for microsatellites.

221 Population admixture inferred using SNPs suggested an optimum number of two clusters with **STRUCTURE**,  
222 the first consisting of AL, GA, and LA; the second with FL by itself (Fig. S3, Supporting information). For  
223 the full microsatellite dataset, there was an optimum of four clusters: one for each population examined (Fig.  
224 S4, Supporting information). The partial microsatellite dataset had three optimum clusters: the first with  
225 LA; the second with AL and GA; and the third with FL (Fig. S5, Supporting information). PCA analysis  
226 produced four clusters for SNPs and both microsatellite datasets (one for each population, Fig. 3A–3C).

227 Random sampling of SNP loci showed that at least 1,600 SNPs were needed to obtain a significant correla-  
228 tion between SNP- and the full microsatellite dataset for allelic richness (Fig. S6A, Supporting information).  
229 Nearly 800 SNPs were needed for expected heterozygosity (Fig. S6B, Supporting information), but only 100  
230 SNPs were needed for SNP- and microsatellite-derived  $F_{ST}$  values to be correlated (Fig. S6C). There was  
231 a similar pattern for the partial microsatellite dataset for allelic richness, expected heterozygosity, and  $F_{ST}$ ,

where at least 800, 800, and 100 SNPs were needed for significant correlations, respectively (Fig. S7A–7C, Supporting information). Parameter variability decreased as the number of randomly chosen SNPs increased, especially after 200, 100, 40, and 40 SNPs for allelic richness, observed and expected heterozygosity, and  $F_{ST}$  values respectively (Fig. S6, Fig. S7, Supporting information).

Effective population sizes estimated using the full microsatellite dataset were not particularly informative, especially the estimates of infinite population sizes from the heterozygous-excess and linkage disequilibrium methods (Fig. S8A, Supporting information). Minus the FL population’s estimate of infinite effective population size, the molecular coancestry method suggested more reasonable estimates of effective population sizes between 34–589 individuals per population. Effective population sizes estimated using immune gene SNPs were more realistic with the heterozygous-excess method suggesting between 133–186 tortoises, and the molecular coancestry method suggesting between 319–427 tortoises per population (Fig. S8B, Supporting information). The linkage disequilibrium method was not informative as all effective population sizes were estimated to be infinite.

The  $N_e$  estimates that ranged between 34–589 individuals (microsatellite and SNP molecular coancestry and SNP heterozygous-excess approaches) suggest that selection coefficients for SNPs would need to be less than 0.1% for genetic drift to outweigh selection.

## Discussion

Estimates of genetic diversity derived from gopher tortoise immunome SNPs and both microsatellite datasets were typically correlated. Given that most gopher tortoise populations are small, immune gene SNPs may be behaving like effectively neutral loci. Thus, these correlations are theoretically reasonable and may hold true for other small populations, for example, endangered and threatened species generally.

Other studies have observed similar and contrasting correlations between SNP and microsatellite-derived estimates of genetic diversity. For example, previous work using 7 SNPs/indels and 14 microsatellites found that expected heterozygosity and allelic richness are positively correlated between the two types of markers in Atlantic salmon populations (Ryynanen *et al.*, 2007). On the contrary, SNP ( $n=1-46$ ) and microsatellite ( $n=10-27$ ) heterozygosities are not correlated for European and North American wolf populations (Vali *et al.*, 2008). Likewise, microsatellite-estimated diversity is different between *Bombus* bumble bee species, but similar when using RADseq loci (Lozier, 2014), thus diversity estimates from these two markers are not correlated.

In gopher tortoises, the rank order for allelic richness and observed heterozygosity was similar but not the

262 same for immune gene SNPs and the full and partial microsatellite datasets, respectively. Similar observations  
 263 have been made by other studies including those comparing SNPs and microsatellites in Atlantic salmon  
 264 (Ryynanen *et al.*, 2007). Rank order may be skewed between the markers because microsatellites are poly-  
 265 allelic while SNPs are di-allelic. In particular, for a microsatellite or SNP marker, there are  $n((n - 1)/2)$   
 266 combinations that result in a heterozygote where  $n$  is the number of alleles. Thus, for a di-allelic marker,  
 267 there is only one combination of alleles that results in a heterozygote, and for a microsatellite that has at  
 268 least 5 alleles (i.e., the average allelic richness for our 10 microsatellites in the full microsatellite dataset),  
 269 there are 10 combinations of alleles that are heterozygous. This could explain why observed heterozygosity  
 270 was not correlated between SNPs and microsatellites for the partial microsatellite dataset.

271 Previous work with microsatellites showed that genetic variation was lower in western versus eastern  
 272 *G. polyphemus* populations (Ennen *et al.*, 2010), and our results with the SNP and re-analysis of the full  
 273 microsatellite datasets support this finding. For the partial microsatellite dataset, the FL and not LA  
 274 population had the lowest observed heterozygosity, but in the full microsatellite dataset, the LA population  
 275 had the lowest observed heterozygosity. The full microsatellite dataset probably provides better estimates  
 276 as 36 and 19 tortoises were analyzed for the LA and FL populations, respectively as compared to just four  
 277 tortoises in the partial microsatellite dataset, therefore observed heterozygosity is likely lower in the LA  
 278 than FL population. Because we only sampled a single western population (Fig. 1), it is not appropriate to  
 279 generalize all western populations as genetically depauperate. Ultimately, additional sampling and immunome  
 280 sequencing from other western *G. polyphemus* populations is warranted.

## 281 Genetic differentiation

282 We also observed strong correlations between SNP and microsatellite-derived genetic differentiation, al-  
 283 beit the order of least to most differentiated comparisons varied. The same was observed for SNP- and  
 284 microsatellite-derived  $F_{ST}$  estimates from four populations of western corn rootworms (Coates *et al.*, 2009).  
 285 The incongruence in rank order may have occurred in both scenarios because of homoplasy issues with mi-  
 286 crosatellites, where high mutation rates can cause repeat number to revert to a particular allele size, which  
 287 can then inflate estimates of gene flow (Coates *et al.*, 2009).

## 288 Genetic admixture

289 Population admixture assessments had few inconsistencies between SNPs and microsatellites. Both PCAs  
 290 suggested four clusters using either marker. We did observe differences in **STRUCTURE** admixture results with

the optimum number of clusters being 2 for SNPs and 4 and 3 for the full and partial microsatellite datasets. Morin *et al.* (2012) compared 42 SNPs versus 22 microsatellites in bowhead whales and also found that the optimum number of clusters is different when using STRUCTURE. SNPs and microsatellites may have suggested different estimates of the optimum number of clusters because some of the SNPs may represent functional rather than neutral genetic variation like the microsatellites, with both types of markers differing to what extent they have been influenced by selection and/or genetic drift.

## Experimental design considerations

So far, we have discussed how population genetic parameters estimated from immune gene SNPs mirror patterns estimated from microsatellite loci, but marker choice also depends on additional considerations such as cost, number of loci, computational issues with NGS generated SNPs, and neutral versus selective processes. First, although sequencing costs are decreasing, NGS techniques can be more expensive than microsatellites on a per sample basis depending on availability of equipment. In particular, the NGS technique used in this paper, in-solution hybridization, requires synthesis of expensive RNA baits/probes, in the order of several thousand dollars (USD). Although tagged microsatellite primers are not trivial in cost, they are far cheaper than biotinylated RNA baits. Further, most genetics labs are not equipped for NGS workflows that require specialized equipment, so lab work must either be outsourced to commercial or non-commercial core facilities.

The number of loci required to adequately address the genetic question at hand is also an important consideration when choosing between SNPs and microsatellites and will vary depending on the question being asked. In general, simulations suggest many more SNPs are needed than microsatellite loci when trying to achieve similar statistical power or parameter estimates. For example, between 60–100 SNP loci are needed for accurate parentage assignment (Anderson & Garza, 2006), and empirical data from sockeye salmon suggest 80 SNPs have higher assignment success and are more accurate for parentage assignment than 11 microsatellites (Hauser *et al.*, 2011). Furthermore, a similar number of SNPs is needed for detecting low levels of divergence (i.e.,  $F_{ST} < 0.005$ ) (Morin *et al.*, 2009). Ryynanen *et al.* (2007) observed significant correlations between 7 SNPs/indels and 14 microsatellite loci when estimating  $F_{ST}$ . Our data subsampling results suggest at least 100 SNP loci are needed for correlating SNP and microsatellite-derived  $F_{ST}$ . For allelic richness and heterozygosities, our data suggest more than 800 SNP loci are needed to correlate with 10 microsatellite loci in *G. polyphemus*, but Ryynanen *et al.* (2007) only needed 7 SNP/indel loci to obtain similar correlations, possibly because they analyzed 21 populations. Acquiring data from a large number of SNPs is not a problem with NGS approaches. Not all SNP loci are equally informative, and smaller SNP

panels may occasionally perform well in comparison to much larger SNP arrays.

Computational issues with NGS are also not trivial, as our own NGS analysis relied on high performance computing resources and required many gigabytes of data storage. This does not include the time or expertise required to write code and scripts to analyze the gigabytes of raw data.

Neutral versus selective processes are also important to consider when deciding between SNPs and microsatellites. Markers such as microsatellites may be neutrally evolving unless linked to functional genes while SNPs could represent both functional and neutral markers and be influenced by both neutral and adaptive processes. Our SNP data had very few SNPs that were putatively under selection (less than 1%), which is in line with previous NGS studies (e.g., Hohenlohe *et al.*, 2010; Lemay & Russello, 2015; Blanco-Bercial & Bucklin, 2016). This together with the observed correlations between SNPs and microsatellites suggests that most of our SNPs were effectively neutral. The gopher tortoise populations we surveyed appear to have small effective population sizes, likely less than 500 individuals per population, so perhaps the selection coefficients of many of the immune gene SNPs were small enough (i.e., less than 0.1 %) that they behaved as effectively neutral loci.

## Conclusion

As more and more population genetic studies are publishing NGS generated SNPs as opposed to microsatellites, it would be useful to identify patterns between microsatellites and NGS derived SNPs and to appreciate the additional functional information commonly provided by SNPs. One apparent pattern is that high variation observed at microsatellites can translate into high SNP-estimates of genetic diversity (Ryynanen *et al.*, 2007) and vice versa. Further, genetic diversity estimated by allelic richness between microsatellites and SNPs may be a less stable metric than diversity estimated by observed and/or expected heterozygosity as more alleles are present in microsatellites than SNPs. This does not mean allelic richness should be ignored especially for conservation purposes because some traits including disease resistance are associated with particular alleles (e.g., Langefors *et al.*, 2001), which is not accounted for by heterozygosity. Another important pattern that may be observed between microsatellites and SNP studies is presence/absence of genetic structure, with any potential inconsistencies resulting from different evolutionary forces acting on the markers. The addition of adaptive processes acting on SNPs can result in similar but disparate structure patterns between the two marker types. Finally, even SNPs that are putatively influenced by selection may behave as effectively neutral loci when effective population sizes are small, thus we recommend researchers consider when comparing population genetic results derived from potentially functional and neutral markers

351 in small populations such as those of threatened and endangered species.

## 352 Acknowledgements

353 This material is based upon work that is supported by the National Institute of Food and Agriculture, U.S.  
354 Department of Agriculture, McIntire Stennis project LAB04066 and LAB94169. The Lucius Gilbert Foun-  
355 dation provided support for sequencing and for J.P.E. We are grateful to Richard Carmouche of Pennington  
356 Biomedical Research Center’s Genomic Core Facility for performing next-generation sequencing laboratory  
357 work. This project/work used genomics core facilities that are supported in part by COBRE (NIH 8 P20  
358 GM103528) and NORC (NIH 2P30DK072476) center grants from the National Institutes of Health. We  
359 appreciate the access we had to the LSU High Performance Computing resources, which we used to analyze  
360 next-generation sequencing data.

## 361 References

- 362 Allendorf FW, Hohenlohe PA, Luikart G (2010) Genomics and the future of conservation genetics. *Nature*  
363 *Reviews Genetics*, **11**, 697–709.
- 364 Anderson EC, Garza JC (2006) The power of single-nucleotide polymorphisms for large-scale parentage  
365 inference. *Genetics*, **172**, 2567–2582.
- 366 Benjamini Y, Hochberg Y (1995) Controlling the false discovery rate: A practical and powerful approach to  
367 multiple testing. *Journal of the Royal Statistical Society. Series B (Methodological)*, **57**, 289–300.
- 368 Bernatchez L, Landry C (2003) MHC studies in nonmodel vertebrates: what have we learned about natural  
369 selection in 15 years? *Journal of Evolutionary Biology*, **16**, 363–377.
- 370 Blanco-Bercial L, Bucklin A (2016) New view of population genetics of zooplankton: RAD-seq analysis reveals  
371 population structure of the North Atlantic planktonic copepod *Centropages typicus*. *Molecular Ecology*,  
372 **25**, 1566–80.
- 373 Bolger AM, Lohse M, Usadel B (2014) TRIMMOMATIC: a flexible trimmer for Illumina sequence data.  
374 *Bioinformatics*, p. btu170.
- 375 Browning SR, Browning BL (2007) Rapid and accurate haplotype phasing and missing-data inference for  
376 whole-genome association studies by use of localized haplotype clustering. *American Journal of Human*  
377 *Genetics*, **81**, 1084–97.
- 378 Clostio RW, Martinez AM, LeBlanc KE, Anthony NM (2012) Population genetic structure of a threatened  
379 tortoise across the south-eastern United States: implications for conservation management. *Animal Con-*  
380 *servation*, **15**, 613–625.
- 381 Coates BS, Sumerford DV, Miller NJ, *et al.* (2009) Comparative performance of single nucleotide polymor-  
382 phism and microsatellite markers for population genetic analysis. *Journal of Heredity*, **100**, 556–564.
- 383 Danecek P, Auton A, Abecasis G, *et al.* (2011) The Variant Call Format and VCFtools. *Bioinformatics*, **27**,  
384 2156–8.

385 De Wit P, Pespeni MH, Ladner JT, *et al.* (2012) The simple fool’s guide to population genomics via RNA-Seq:  
386 an introduction to high-throughput sequencing data analysis. *Molecular Ecology Resources*, **12**, 1058–67.

387 DeFaveri J, Viitaniemi H, Leder E, Meril   J (2013) Characterizing genic and nongenic molecular markers:  
388 comparison of microsatellites and SNPs. *Molecular Ecology Resources*, **13**, 377–392.

389 Do C, Waples RS, Peel D, Macbeth G, Tillett BJ, Ovenden JR (2014) NeEstimator v2: re-implementation  
390 of software for the estimation of contemporary effective population size (Ne) from genetic data. *Molecular*  
391 *Ecology Resources*, **14**, 209–214.

392 Earl DA, vonHoldt BM (2012) STRUCTURE HARVESTER: a website and program for visualizing STRUC-  
393 TURE output and implementing the Evanno method. *Conservation Genetics Resources*, **4**, 359–361.

394 Elbers JP, Taylor SS (2015) GO2TR: a gene ontology-based workflow to generate target regions for target  
395 enrichment experiments. *Conservation Genetics Resources*, **7**, 851–857.

396 Enge K, Berish J, Bolt R, Dziergowski A, Musinsky H (2006) Biological status report gopher tortoise. Report,  
397 Florida Fish and Wildlife Conservation Commission.

398 Ennen JR, Kreiser BR, Qualls CP (2010) Low genetic diversity in several gopher tortoise (*Gopherus polyph-*  
399 *mus*) populations in the Desoto National Forest, Mississippi. *Herpetologica*, **66**, 31–38.

400 Excoffier L, Lischer HE (2010) Arlequin suite ver 3.5: a new series of programs to perform population genetics  
401 analyses under Linux and Windows. *Molecular Ecology Resources*, **10**, 564–7.

402 Foll M, Gaggiotti O (2008) A genome-scan method to identify selected loci appropriate for both dominant  
403 and codominant markers: a Bayesian perspective. *Genetics*, **180**, 977–993.

404 Frankham R, Ballou JD, Briscoe DA (2010) *Introduction to conservation genetics*. Cambridge University  
405 Press, Cambridge, 2nd edn..

406 Garke C, Ytournal F, Bedhom B, *et al.* (2012) Comparison of SNPs and microsatellites for assessing the  
407 genetic structure of chicken populations. *Animal Genetics*, **43**, 419–428.

408 Glover KA, Hansen MM, Lien S, Als TD, Hoyheim B, Skaala O (2010) A comparison of SNP and STR loci  
409 for delineating population structure and performing individual genetic assignment. *BMC Genetics*, **11**,  
410 1–12.

411 Goudet J (2005) HIERFSTAT, a package for R to compute and test hierarchical F-statistics. *Molecular*  
412 *Ecology Notes*, **5**, 184–186.

413 Grueber CE, Wallis GP, Jamieson IG (2013) Genetic drift outweighs natural selection at toll-like receptor  
414 (TLR) immunity loci in a re-introduced population of a threatened species. *Molecular Ecology*, **22**, 4470–82.

415 Gupta P, Roy J, Prasad M (2001) Single nucleotide polymorphisms SNPs: a new paradigm in molecular  
416 marker technology and DNA polymorphism detection with emphasis on their use in plants. *Current*  
417 *Science*, **80**, 524–535.

418 Hauser L, Baird M, Hilborn RAY, Seeb LW, Seeb JE (2011) An empirical comparison of SNPs and microsatel-  
419 lites for parentage and kinship assignment in a wild sockeye salmon (*Oncorhynchus nerka*) population.  
420 *Molecular Ecology Resources*, **11**, 150–161.

421 Hedrick PW (1999) Balancing selection and MHC. *Genetica*, **104**, 207–214.

422 Hohenlohe PA, Bassham S, Etter PD, Stiffler N, Johnson EA, Cresko WA (2010) Population genomics of  
423 parallel adaptation in threespine stickleback using sequenced RAD tags. *PLoS Genetics*, **6**, e1000862.

424 Hubisz MJ, Falush D, Stephens M, Pritchard JK (2009) Inferring weak population structure with the assis-  
425 tance of sample group information. *Molecular Ecology Resources*, **9**, 1322–32.

426 Jeffries DL, Copp GH, Lawson Handley L, Olsen KH, Sayer CD, Hanfling B (2016) Comparing RADseq and  
427 microsatellites to infer complex phylogeographic patterns, an empirical perspective in the Crucian carp,  
428 *Carassius carassius*, L. *Molecular Ecology*, p. in press.

429 Kopelman NM, Mayzel J, Jakobsson M, Rosenberg NA, Mayrose I (2015) CLUMPAK: a program for identify-  
430 ing clustering modes and packaging population structure inferences across k. *Molecular Ecology Resources*,  
431 **15**, 1179–91.

432 Kuo CH, Moran NA, Ochman H (2009) The consequences of genetic drift for bacterial genome complexity.  
433 *Genome Research*, **19**, 1450–1454.

434 Langefors A, Lohm J, Grahn M, Andersen O, von Schantz T (2001) Association between major histocompat-  
435 ibility complex class iiB alleles and resistance to *Aeromonas salmonicida* in atlantic salmon. *Proceedings of*  
436 *the Royal Society of London B*, **268**, 479–485.

437 Lemay MA, Russello MA (2015) Genetic evidence for ecological divergence in kokanee salmon. *Molecular*  
438 *Ecology*, **24**, 798–811.

439 Li C, Sun Y, Huang HW, Cannon CH (2014) Footprints of divergent selection in natural populations of  
440 *Castanopsis fargesii* (Fagaceae). *Heredity*, **113**, 533–41.

441 Li H (2013) Aligning sequence reads, clone sequences and assembly contigs with BWA-MEM. *arXiv*,  
442 **1303.3997**.

443 Li H, Durbin R (2009) Fast and accurate short read alignment with Burrows-Wheeler transform. *Bioinfor-*  
444 *matics*, **25**, 1754–60.

445 Li H, Handsaker B, Wysoker A, *et al.* (2009) The Sequence Alignment/Map format and SAMtools. *Bioin-*  
446 *formatics*, **25**, 2078–9.

447 Li YC, Korol AB, Fahima T, Beiles A, Nevo E (2002) Microsatellites: genomic distribution, putative functions  
448 and mutational mechanisms: a review. *Molecular Ecology*, **11**, 2453–2465.

449 Liao Y, Smyth GK, Shi W (2014) featureCounts: an efficient general purpose program for assigning sequence  
450 reads to genomic features. *Bioinformatics*, **30**, 923–30.

451 Lischer H, Excoffier L (2012) PGDSpider: an automated data conversion tool for connecting population  
452 genetics and genomics programs. *Bioinformatics*, **28**, 298–299.

453 Lozier JD (2014) Revisiting comparisons of genetic diversity in stable and declining species: assessing genome-  
454 wide polymorphism in North American bumble bees using RAD sequencing. *Molecular Ecology*, **23**, 788–  
455 801.

456 Lunter G, Goodson M (2011) STAMPY: a statistical algorithm for sensitive and fast mapping of Illumina  
457 sequence reads. *Genome Research*, **21**, 936–9.

458 Lynch M, Bobay LM, Catania F, Gout JF, Rho M (2011) The repatterning of eukaryotic genomes by random  
459 genetic drift. *Annual Review of Genomics and Human Genetics*, **12**, 347–366.

460 McKenna A, Hanna M, Banks E, *et al.* (2010) The Genome Analysis Toolkit: a MapReduce framework for  
461 analyzing next-generation DNA sequencing data. *Genome Research*, **20**, 1297–1303.

462 Miller HC, Lambert DM (2004) Genetic drift outweighs balancing selection in shaping postbottleneck major  
463 histocompatibility complex variation in New Zealand robins (Petroicidae). *Molecular Ecology*, **13**, 3709–  
464 3721.

465 Miller HC, Miller KA, Daugherty CH (2008) Reduced MHC variation in a threatened tuatara species. *Animal*  
466 *Conservation*, **11**, 206–214.



467 Morin PA, Archer FI, Pease VL, *et al.* (2012) An empirical comparison of SNPs and microsatellites for  
468 population structure, assignment, and demographic analyses of bowhead whale populations. *Endangered*  
469 *Species Research*, **19**, 129–147.

470 Morin PA, Martien KK, Taylor BL (2009) Assessing statistical power of SNPs for population structure and  
471 conservation studies. *Molecular Ecology Resources*, **9**, 66–73.

472 Moritz C (1994) Applications of mitochondrial DNA analysis in conservation: a critical review. *Molecular*  
473 *Ecology*, **3**, 401–411.

474 Narum SR, Banks M, Beacham TD, *et al.* (2008) Differentiating salmon populations at broad and fine  
475 geographical scales with microsatellites and single nucleotide polymorphisms. *Molecular Ecology*, **17**, 3464–  
476 3477.

477 Niskanen AK, Kennedy LJ, Ruokonen M, *et al.* (2014) Balancing selection and heterozygote advantage in  
478 major histocompatibility complex loci of the bottlenecked Finnish wolf population. *Molecular Ecology*, **23**,  
479 875–89.

480 Nomura T (2008) Estimation of effective number of breeders from molecular coancestry of single cohort  
481 sample. *Evolutionary Applications*, **1**, 462–474.

482 Ortutay C, Vihinen M (2006) Immunome: a reference set of genes and proteins for systems biology of the  
483 human immune system. *Cellular Immunology*, **244**, 87–89.

484 Pritchard JK, Stephens M, Donnelly P (2000) Inference of population structure using multilocus genotype  
485 data. *Genetics*, **155**, 945–959.

486 R Core Team (2015) *R: A Language and Environment for Statistical Computing*. R Foundation for Statistical  
487 Computing, Vienna, Austria.

488 Ryynanen HJ, Tonteri A, Vasemagi A, Primmer CR (2007) A comparison of biallelic markers and microsatel-  
489 lites for the estimation of population and conservation genetic parameters in Atlantic salmon (*Salmo salar*).  
490 *Journal of Heredity*, **98**, 692–704.

491 Shaffer HB, Minx P, Warren DE, *et al.* (2013) The western painted turtle genome, a model for the evolution  
492 of extreme physiological adaptations in a slowly evolving lineage. *Genome Biology*, **14**, R28.

493 Sommer S (2005) The importance of immune gene variability (MHC) in evolutionary ecology and conservation.  
494 *Frontiers in Zoology*, **2**, 16–16.

495 Taylor SS, Jenkins DA, Arcese P (2012) Loss of MHC and neutral variation in Peary caribou: genetic drift  
496 is not mitigated by balancing selection or exacerbated by MHC allele distributions. *PLoS One*, **7**, e36748.

497 Vali U, Einarsson A, Waits L, Ellegren H (2008) To what extent do microsatellite markers reflect genome-wide  
498 genetic diversity in natural populations? *Molecular Ecology*, **17**, 3808–3817.

499 Vasemagi A, Gross R, Paaver T, Koljonen ML, S  is   M, Nilsson J (2005) Analysis of gene associated  
500 tandem repeat markers in atlantic salmon (*salmo salar* l.) populations: implications for restoration and  
501 conservation in the baltic sea. *Conservation Genetics*, **6**, 385–397.

502 Waples RS, Do C (2008) LDNE: a program for estimating effective population size from data on linkage  
503 disequilibrium. *Molecular Ecology Resources*, **8**, 753–756.

504 Weber DS, Stewart BS, Schienman J, Lehman N (2004) Major histocompatibility complex variation at three  
505 class II loci in the northern elephant seal. *Molecular Ecology*, **13**, 711–718.

506 Wright S (1931) Evolution in mendelian populations. *Genetics*, **16**, 97–159.

507 Zhdanova OL, Pudovkin AI (2008) Nb\_HetEx: a program to estimate the effective number of breeders.  
508 *Journal of Heredity*, **99**, 694–695.

## Data Accessibility

Raw sequencing data are available from the Sequence Read Archive (accession: SRP061247). BAM and VCF files are available from Dryad repository (doi: 10.5061/dryad.40c7c). Detailed analytical methods and scripts to create Tables and Figures are available from [https://github.com/jelber2/immunome\\_2014](https://github.com/jelber2/immunome_2014).

## Author Contributions

J.P.E. designed the study and performed SNP analyses. R.W.C. performed microsatellite analyses. J.P.E. and S.S.T. wrote the paper.

## Supporting Information

Additional Supporting Information may be found in the online version of this article:

**Table S1** Sequencing metrics for *Gopherus polyphemus* samples. Percent UR for percent of total reads that were unique, Percent URA for percent of unique reads that were alignable, Mean coverage for mean number of reads across the target region, Percent 20x for percent of bases in target region with greater than 20x coverage, No. genes for number of genes, and No. exons for number of exons.

**Table S2** All genes with di-allelic, polymorphic SNPs from 16 *Gopherus polyphemus* samples.

**Fig. S1** Coverage plots for first eight *Gopherus polyphemus* samples showing number of sequencing reads at or above specified proportions. A value at 100 Depth and 0.5 fraction means 50 percent of bases were at or above 100X coverage.

**Fig. S2** Coverage plots for last eight *Gopherus polyphemus* samples showing number of sequencing reads at or above specified proportions.

**Fig. S3** STRUCTURE plot for 16 *Gopherus polyphemus* sequenced at 17,901 immune gene SNPs with optimum number of clusters  $K = 2$  determined by STRUCTURE HARVESTER.

**Fig. S4** STRUCTURE plot for the full microsatellite dataset (101 *Gopherus polyphemus* genotyped at 10 microsatellite loci) with optimum number of clusters  $K = 4$  determined by STRUCTURE HARVESTER.

**Fig. S5** STRUCTURE plot for the partial microsatellite dataset (16 *Gopherus polyphemus* genotyped at 10 microsatellite loci) with optimum number of clusters  $K = 3$  determined by STRUCTURE HARVESTER.

**Fig. S6** Subsampling analysis showing how many randomly sampled SNP loci out of the total of 17,901 are needed in comparison to the full microsatellite dataset (101 *Gopherus polyphemus* genotyped at 10 microsatel-

536 lite loci) for Pearson's  $r$  correlation coefficient to be significant at 0.05 level (dotted line) for (A) observed  
537 heterozygosity; (B) expected heterozygosity; and (C)  $F_{ST}$ . There were 10 simulations for each size class of  
538 SNPs.  $H_O$  for observed heterozygosity,  $H_E$  for expected heterozygosity.

539 **Fig. S7** Subsampling analysis showing how many randomly sampled SNP loci out of the total of 17,901  
540 are needed in comparison to the partial microsatellite dataset (16 *Gopherus polyphemus* genotyped at 10 mi-  
541 crosatellite loci) for Pearson's  $r$  correlation coefficient to be significant at 0.05 level (dotted line) for (A) allelic  
542 richness; (B) expected heterozygosity; and (C)  $F_{ST}$ . There were 10 simulations for each size class of SNPs.  
543  $A_R$  for allelic richness,  $H_E$  for expected heterozygosity.

544 **Fig. S8** Effective population sizes per generation ( $N_e$ ) along with 95 % confidence intervals for *Gopherus*  
545 *polyphemus* samples estimated with the program **NeEstimator** using (A) the full microsatellite dataset (101  
546 *G. polyphemus* genotyped at 10 microsatellite loci) or (B) the SNP dataset (16 *G. polyphemus* sequenced at  
547 17,901 immune gene SNPs). Dots that are on the top of the graph represent  $N_e$  estimates of infinity, and  
548 lines that extend to the top of the graph represent upper 95 % confidence limits of infinity. LD for linkage  
549 disequilibrium method of Waples & Do (2008), HET for heterozygote-excess method of Zhdanova & Pudovkin  
550 (2008), and MOL for the molecular coancestry method of Nomura (2008). Note that the HET and MOL  
551 methods estimate the effective number of breeders per year ( $N_b$ ), which were converted to  $N_e$  by multiplying  
552  $N_b$  by the generation time of 31 years for *G. polyphemus* (Enge et al. 2006).

553

# Tables and Figures

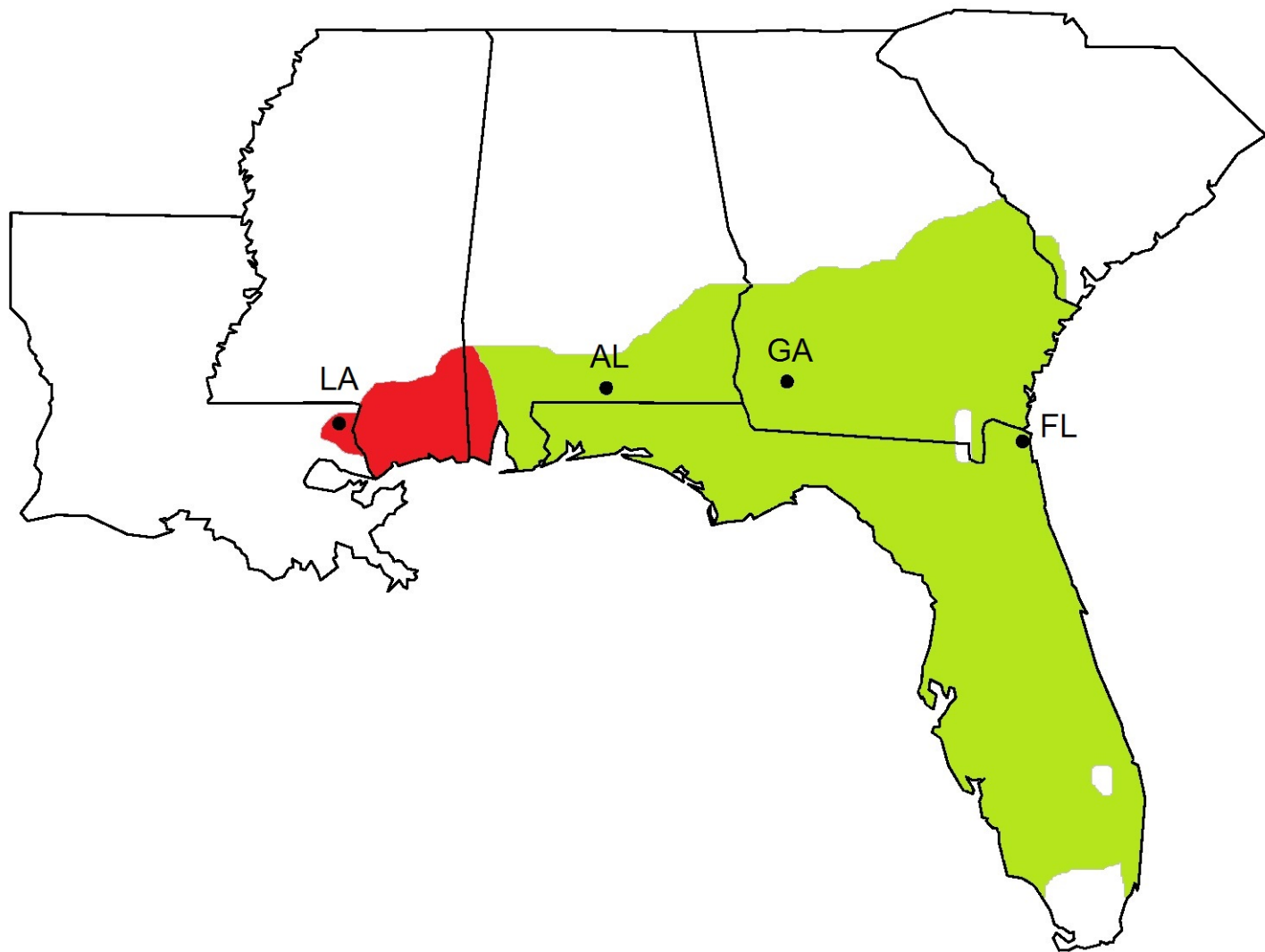
**Table 1** Comparisons of full (101 individuals) and partial (16 individuals) microsatellite datasets with SNP dataset (16 individuals) for *Gopherus polyphemus*. Values with decimals represent mean population genetic parameter values. AR for allelic richness, Ho for observed heterozygosity, HE for expected heterozygosity, No. pops for number of optimum populations determined with STRUCTURE HARVESTER for STRUCTURE or visually for PCA.

Variable	SNP dataset	Full Microsatellite Dataset	Partial Microsatellite Dataset
AR	1.541	5.487	2.900
Correlation with SNPs		not significant	not significant
Ho	0.267	0.495	0.469
Correlation with SNPs		significant	not significant
HE	0.228	0.543	0.531
Correlation with SNPs		significant	significant
FST	0.282	0.336	0.320
Correlation with SNPs		significant	significant
No. pops STRUCTURE	2	4	3
No. pops PCA	4	4	4

561 **Table 2** Histocompatibility and Toll-like Receptor Loci with di-allelic, polymorphic SNPs in the *Gopherus*  
562 *polyphemus* SNP dataset (16 *G. polyphemus* sequenced at 17,901 immune gene SNPs).

Histocompatibility Loci
CD74 molecule, major histocompatibility complex, class II invariant chain
Class I histocompatibility antigen, F10 alpha chain-like
Class II histocompatibility antigen, M alpha chain
Class II, major histocompatibility complex, transactivator
DLA class II histocompatibility antigen, DR-1 beta chain-like
H-2 class II histocompatibility antigen, A-R alpha chain-like
H-2 class II histocompatibility antigen, E-S beta chain-like
HLA class II histocompatibility antigen, DP alpha 1 chain-like
HLA class II histocompatibility antigen, DR alpha chain-like
HLA class II histocompatibility antigen, DR beta 5 chain-like
HLA class II histocompatibility antigen, DRB1-15 beta chain-like
Major histocompatibility complex class I-related gene protein-like
Rano class II histocompatibility antigen, A beta chain-like
Toll-like Receptor Loci
Toll-like Receptor 13
Toll-like Receptor 2
Toll-like Receptor 7
Toll-like Receptor 8
Toll-like Receptor adaptor molecule 1
Toll-like Receptor adaptor molecule 2

563



564

565 **Fig. 1** *Gopherus polyphemus* range map and sampling sites used in this study. Range of western *G. polyphe-*  
 566 *mus* populations darkly shaded on the left with eastern populations lightly shaded on the right. LA for  
 567 Florida Gas Pipeline, Washington Parish, Louisiana, USA (latitude, longitude, sample size for full microsatel-  
 568 lite dataset = 30.78, -90.00;  $N = 36$ ). AL for Solon Dixon, Andalusia, Alabama, USA (31.16, -86.70;  $N =$   
 569 20). GG for Jones Ecological Research Center, Georgia, USA. (31.23, -84.47;  $N = 26$ ). FL for Private Site,  
 570 Nassau County, Florida, USA (30.59, -81.56;  $N = 19$ ).

571

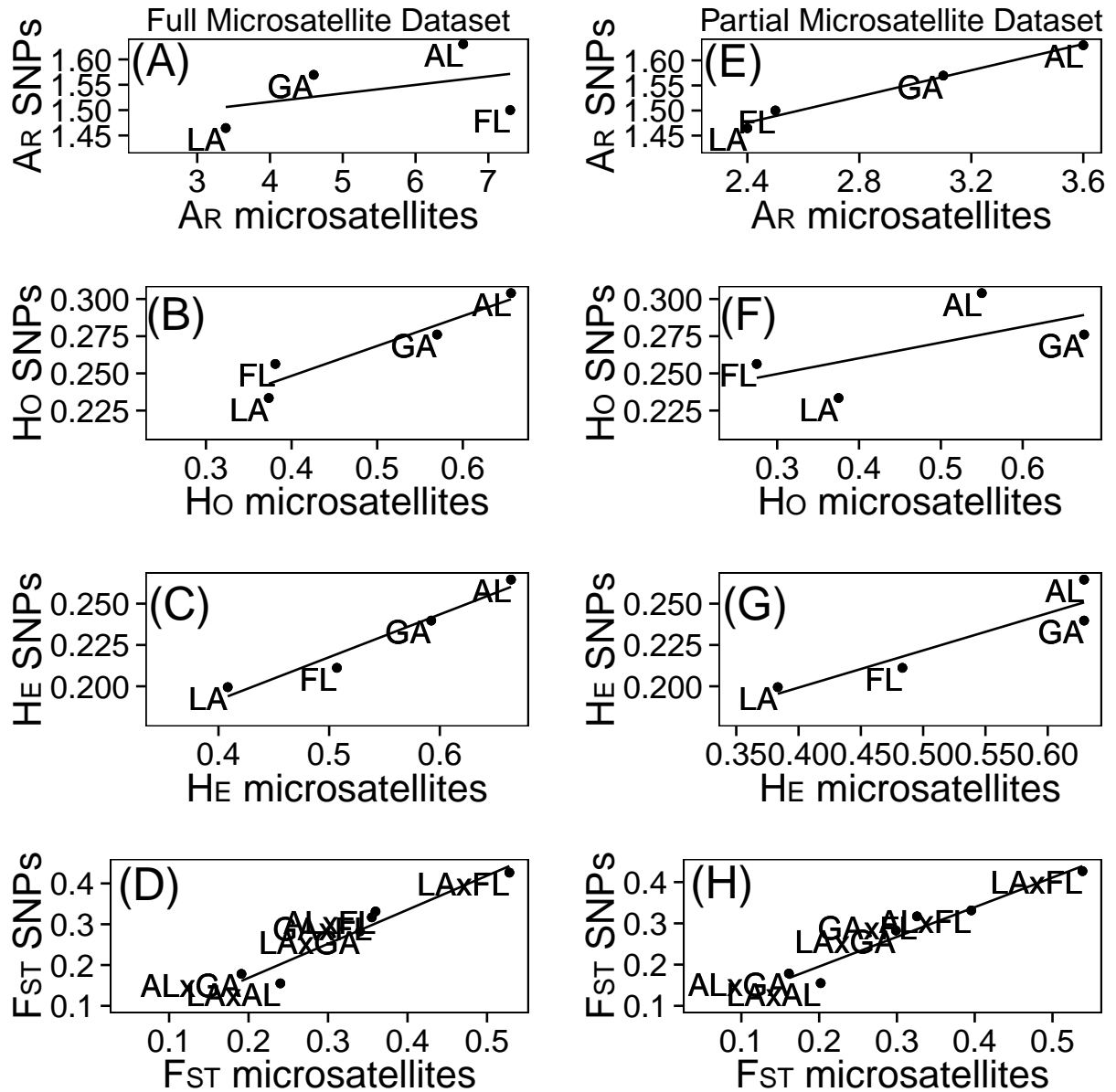


**Fig. 2** Correlations between 10 microsatellites and 17,901 immune gene SNPs for *Gopherus polyphemus* samples. Left column for full microsatellite dataset (101 *G. polyphemus* genotyped at 10 microsatellites) for (A) allelic richness, Pearson's  $r = 0.411$ ,  $P = 0.294$ ; (B) observed heterozygosity, Pearson's  $r = 0.945$ ,  $P = 0.028$ ; (C) expected heterozygosity, Pearson's  $r = 0.976$ ,  $P = 0.012$ ; and (D) FST, Pearson's  $r = 0.96$ ,  $P = 0.001$ . Right column for partial microsatellite dataset (16 *G. polyphemus* genotyped at 10 microsatellites) for (E) allelic richness, Pearson's  $r = 0.992$ ,  $P = 0.004$ ; (F) observed heterozygosity, Pearson's  $r = 0.63$ ,  $P = 0.185$ ; (G) expected heterozygosity, Pearson's  $r = 0.924$ ,  $P = 0.038$ ; and (H) FST, Pearson's  $r = 0.968$ ,  $P = 0.001$ . AR for allelic richness, Ho for observed heterozygosity, He for expected heterozygosity.

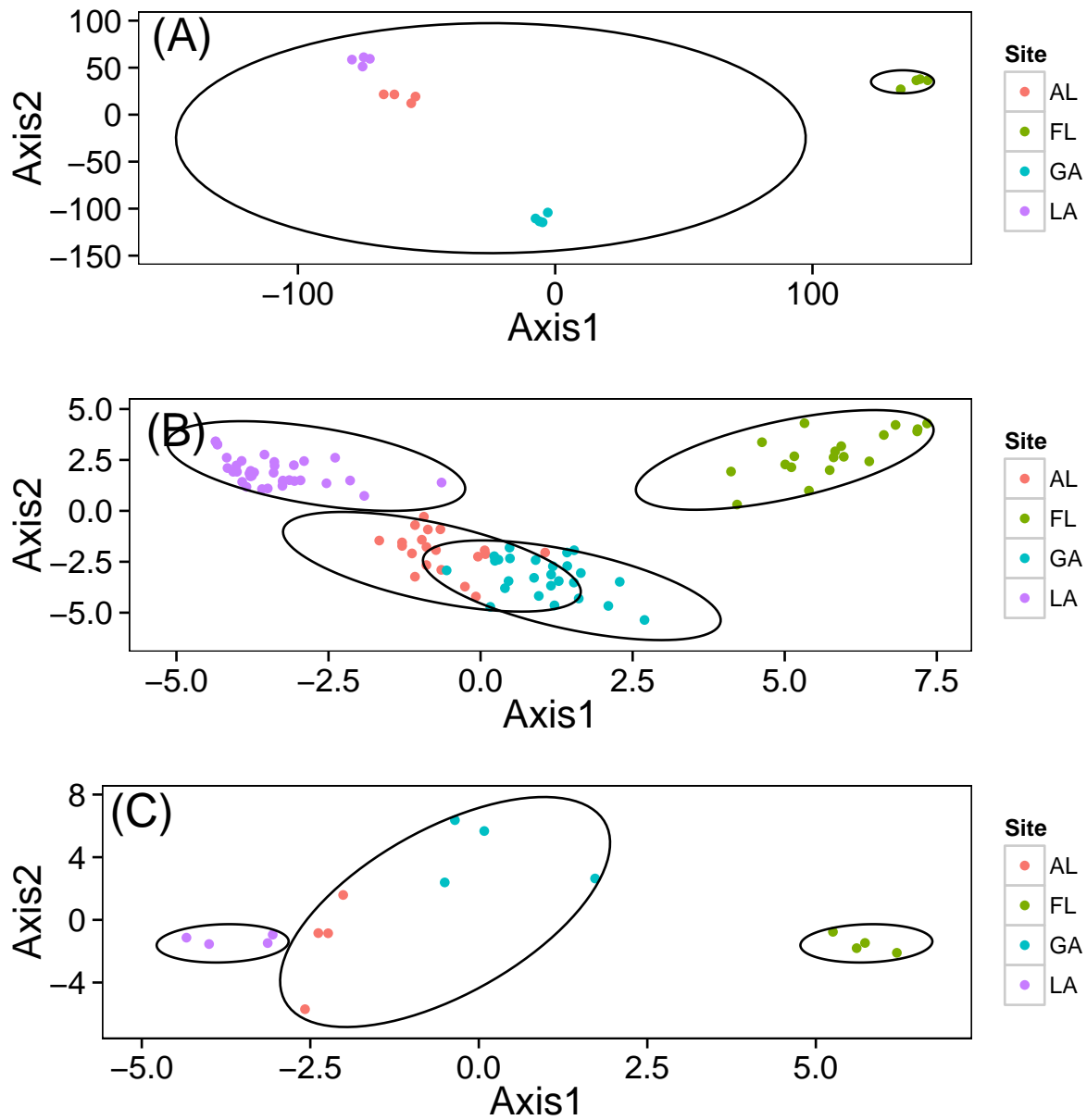


**Fig. 3** Principle component analysis for *Gopherus polyphemus* datasets: (A) the SNP dataset (16 *G. polyphemus* sequenced at 17,901 immune gene SNPs); (B) full microsatellite dataset (101 *G. polyphemus* genotyped at 10 microsatellites); and (C) partial microsatellite dataset (16 *G. polyphemus* genotyped at 10 microsatellites). Circles indicate optimum clusters identified using STRUCTURE and STRUCTURE HARVESTER.